Initial study on thermal stability of cold spray tantalum coating irradiated with deuterium for fusion applications

Mykola Ialovega, Tyler Dabney, Marcos Navarro Gonzalez, Hwasung Yeom, Danah Velez, Evan Willing, Jay K Anderson, Thierry Angot, Régis Bisson, Cary Forest, et al.

Initial study on thermal stability of cold spray tantalum coating irradiated with deuterium for fusion applications

Physica Scripta

PAPER

Initial study on thermal stability of cold spray tantalum coating irradiated with deuterium for fusion applications

Mykola Ialovega[1], **Tyler Dabney**[1], **Marcos Navarro Gonzalez**[1], **Hwasung Yeom**[1,2], **Danah Velez**[1], **Evan Willing**[1], **Jay K Anderson**[3], **Thierry Angot**[4], **Régis Bisson**[4], **Cary Forest**[3], **Arkadi Kreter**[5], **Oliver Schmitz**[1] and **Kumar Sridharan**[1]

[1] University of Wisconsin-Madison, Department of Engineering Physics, 1500 Engineering Drive, 53706 Madison, WI, United States of America
[2] Pohang University of Science and Technology, Division of Advanced Nuclear Engineering, 37673 Pohang, Republic Of Korea
[3] University of Wisconsin-Madison, Department of Physics, 1150 University Ave., 53706 Madison, WI, United States of America
[4] Aix Marseille Univ., CNRS, PIIM, UMR 7345, 13013 Marseille, France
[5] Forschungszentrum Jülich GmbH, IEK-4, 52425 Jülich, Germany

E-mail: ialovega@wisc.edu

Keywords: tantalum, deuterium plasma irradiation, cold spray deposition, thermal cycling, XPS, XRD, deuterium retention

OPEN ACCESS

RECEIVED
1 June 2023

REVISED
1 October 2023

ACCEPTED FOR PUBLICATION
5 October 2023

PUBLISHED
17 October 2023

Abstract

Removal of neutral hydrogen atoms in the plasma edge reduces the number of charge exchange events and thus, the net energy losses in the plasma, significantly improving performance of fusion devices. Effective control of the residual pressure of hydrogen isotopes (HIs) in the plasma edge may be achieved by utilizing a hydrogen absorbing first wall interface capable of withstanding the harsh fusion environment. In this study, we have investigated tantalum (Ta) coating deposited by cold spray technology on 316L stainless steel substrate as a potential plasma-facing material surface. High fluence low energy deuterium plasma irradiation experiments and subsequent thermal annealing cycles associated with thermal desorption spectrometry (TDS) demonstrated superior structural stability of the Ta coating. TDS experiments revealed the outgassing of deuterium (as measure of its retention) for cold spray Ta coatings to be three times higher than bulk Ta and two orders of magnitude greater than bulk polycrystalline W. X-ray photoelectron spectroscopy revealed evolution of oxidation states upon deuterium irradiation and a partial recovery of the metallic signature of Ta after the thermal treatment at 1100 K.

1. Introduction

The need for high vacuum is widespread in scientific and industrial applications (e.g. electron microscopes, particle accelerators, gravitational wave detectors, facilities simulating interstellar space as well as processing of advanced semiconductor devices, nuclear industry, metallurgy, food industry, etc). Reduction of the hydrogen isotopes (HIs) outgassing rate is a most challenging problem for achieving a pressure below the ultrahigh vacuum ($<10^{-6}$ Pa) in the devices utilizing metallic walls [1]. Overcoming this challenge also helps in reduction of residual water in vacuum systems operating at a higher pressure [2].

High vacuum and control of residual hydrogen pressure is of particular importance for laboratory fusion devices in which the vacuum vessel first wall is subjected to significant fluxes of high-energy hydrogen ions and neutrals, as well as to large heat loads. For example, the successful performance of the Wisconsin High-temperature-superconducting Axisymmetric Mirror experiment (WHAM) [3], a new magnetic mirror device currently under construction which is intended to operate with weakly collisional MHD stable fusion plasma, depends strongly on the effective suppression of energy losses associated with the charge-exchange events (CX). In WHAM, fast sloshing ions H_f^+ generated in plasma by neutral beam injection and radio-frequency heating may exchange electrons with low-energy H neutrals arriving at the plasma edge from the first wall, thus, creating energetic neutrals which escape the magnetic confinement region:

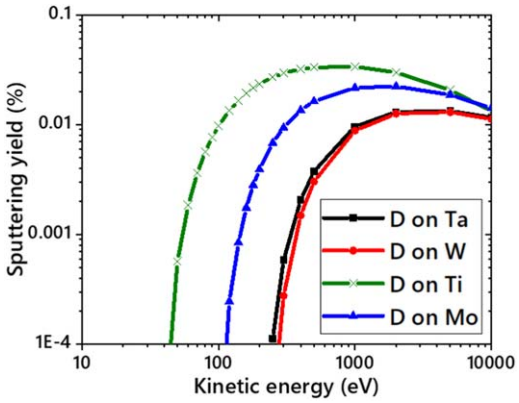

Figure 1. SDTrimSP [16] calculations of sputtering yield as a function of kinetic energy of incident deuterium (D) ions for Ti, Mo, Ta and W target materials under normal incidence.

$$H_f^+ + H \rightarrow H_f + H^+ \quad (1)$$

The pressure of neutrals in the plasma edge can be limited by deposition of an engineered coating on the surface of WHAM's vacuum envelope (first-wall). The coating should be capable of withstanding the harsh environment associated with plasma irradiation and high heat loads. Moreover, functionality of the first-wall should also allow for temperature-controlled desorption of hydrogen isotopes (HIs) thereby increasing the density of neutrals in the plasma edge and ensuring the ability of the Ta coating to free up the trapping sites for hydrogen. If the mechanical integrity and physical properties of the coating are not affected, then this approach would allow for possibility of regeneration of the coating for continued use (wall regeneration). The functional first-wall interface may also benefit the proposed upgrade of the Helically Symmetric eXperiment (HSX) stellarator for testing the non-resonant divertor concept in detached conditions [4].

The cold spray (CS) technology has been used for deposition of high-density coatings of metallic materials for a wide range of applications [5]. In this process, feedstock powder particles of the coating material are propelled at supersonic velocities on to a substrate surface by a preheated gas jet passing through a converging-diverging nozzle. This high velocity impact of the particles on the substrate results in severe high strain rate plastic deformation that facilitates particle-substrate adhesion and inter-particle cohesion by an associated adiabatic shear process. The cold spray deposition process has a number of attributes. The process is carried out at ambient temperatures and pressures and the deposition rates are high. The particle temperature is low and the deposition occurs in solid state and therefore the coatings are devoid of microstructures associated with solidification such as segregation and oxidation, as well as the detrimental effects associated with thermal expansion mismatches between the coating and substrate [5]. Moreover, due to the high impact, the thin native oxide layer on the particles or the substrates is jetted out promoting good metallurgical bonding [6].

The cold spray process was shown to be an effective tool for manufacturing of functional gradient materials for fusion applications [7]. For example, the recent work by Neu *et al* [8] reported the successful deposition of thick mixed tungsten/tantalum coatings capable of withstanding fusion-relevant heat transients (up to 4 MW m^{-2}), suggesting cold spray to be a promising technology for fusion applications. Tantalum (Ta) is a widely used material in chemistry, medical applications, electronics, aerospace and nuclear industry [9] because of its high melting temperature, excellent room-temperature ductility [10] and outstanding corrosion resistance [5, 11]. Ta, similar to titanium (Ti), exhibits exothermic hydrogen absorption which results in a much higher hydrogen isotopes (HIs) inventory compared to other refractory metals such as tungsten (W) and molybdenum (Mo) [12–14]. In addition, the low sputtering rate of Ta by HIs (see figure 1), as well as the high radiation damage resistance of Ta to neutrons and gamma radiation [15], makes it a promising candidate material for the HIs retaining first-wall interface of laboratory fusion devices such as WHAM. Stainless steel (SS) is a reasonable choice for the substrate given its common use in high vacuum devices.

There have been a number of studies on characterization of physical and mechanical properties as well as morphology of cold sprayed Ta coatings [5, 10, 11, 17–19]. In particular, experimental work by Koivuluoto *et al* [17] revealed strong interparticle bonding between Ta particles. Bailly *et al* [19] showed that cold sprayed Ta has a uniform hardness and compressive residual stress across the thickness of the coating at 353K. Kumar *et al* [5] demonstrated disappearance of inter-particle boundaries and pores in cold sprayed Ta coatings after heat treatment at 1773 K due to diffusion effects, making the coating properties comparable to those of bulk Ta. However, it has been shown that Ta subjected to a high dose of HIs and subsequent thermal cycling may result in structural modifications due to a possible formation of various hydride states of Ta [20–22]. Moreover,

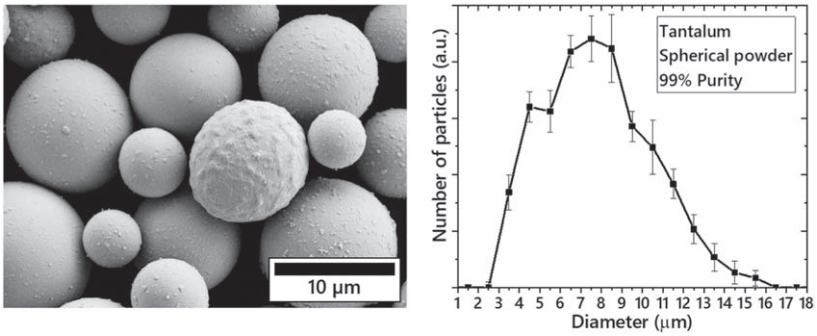

Figure 2. SEM image of tantalum powder and the size distribution of the powder particles used for cold spray.

oxidation of Ta surface may reduce HIs absorption [13, 23] affecting the desired functionality of the coatings as the retaining first-wall material of Plasma-Facing Components (PFCs). Thus, it is important to systematically investigate the evolution of surface and bulk morphology, chemical composition, mechanical properties and retention mechanisms in the cold spray coatings subjected to high hydrogen fluxes and thermal cycling at elevated temperatures matching the expectations for PFCs in fusion devices.

The kinetic energy of CX neutrals in fusion devices can be on the order of several keV which can potentially result in a significant damage and degradation of the first-wall material [24]. In the present study, we have irradiated cold spray Ta coatings with deuterium (D) ions with the kinetic energy below the sputtering threshold (250eV in figure 1) to eliminate creation of the irradiation-induced defects due to the ion impact. Exposure to the high deuterium dose of 3×10^{25} D/m^2 at low temperature of 535 K was performed to achieve saturation of the subsurface Ta layer with D atoms and to evaluate possible surface degradation and blister formation in the coating [14]. Thermal annealing cycles were performed up to 1100 K, close to the maximum recommended operational temperature limit for SS 316L substrate [25] to evaluate the physical and adhesion properties of the coatings associated with outgassing of the retained D from Ta [14]. The chosen irradiation and thermal annealing conditions are also relevant to the divertor region of a tokamak [26], since several studies [12, 14, 27] have suggested that Ta has a potential to serve as the divertor material for ITER if an operational scenario for this plasma-facing material allows for maintaining tritium inventory within tolerable limits.

In this work we report on the development, effects of deuterium plasma irradiation and annealing tests of tantalum coatings deposited using the cold spray technology on SS 316L substrate using a well-defined high-purity Ta powder feedstock. We aim to provide a better understanding of impact-induced cold spray fabrication process for high-Z materials and to expand our knowledge on the behavior of the cold sprayed Ta under high fluence D irradiation and thermal treatment conditions relevant to fusion. For studying practical feasibility of this approach, we also aim to provide the scheme of characterizing the as-deposited cold spray coatings with varying the temperature and speed of the feed-stock powder at the nozzle outlet. The follow-up characterization of the surface and bulk morphology at the microscale, structural and sub-surface chemical composition of the coating after high-temperature annealing, particularly in comparison with bulk Ta coatings, provides the basis for future evaluation of D retention mechanisms in the Ta cold spray coating as a potential hydrogen retaining first-wall interface of WHAM and other fusion devices.

2. Experimental procedures

2.1. Cold spray deposition of tantalum

Commercially available spherical tantalum powder (Stanford Advanced Materials Inc.) with an average particle size of 8 μm was used as feedstock (figure 2). Figure 3(a) shows a schematic illustration of the cold spray system at the University of Wisconsin-Madison [5] that was used for deposition of tantalum coating in this study. The Ta powder was sprayed on SS316L substrate coupon (figure 3(b) which was mechanically polished using 600-grit silicon carbide paper to remove any surface oxide contamination and then ultrasonically cleaned in ethanol bath prior to coating deposition. For spraying, nitrogen gas (N_2) was preheated to 1023 K and the gas pressure was maintained at 3.9 $\pm$ 0.1 MPa. The translation speed of the robotic spray gun equipped with the de Laval nozzle was 400 mm/s. The selection of the deposition parameters was based on previous work on optimization of Ta cold spray coatings [5]. Figure 3(c) shows the surface of the as-deposited coatings on the 316L stainless steel substrate.

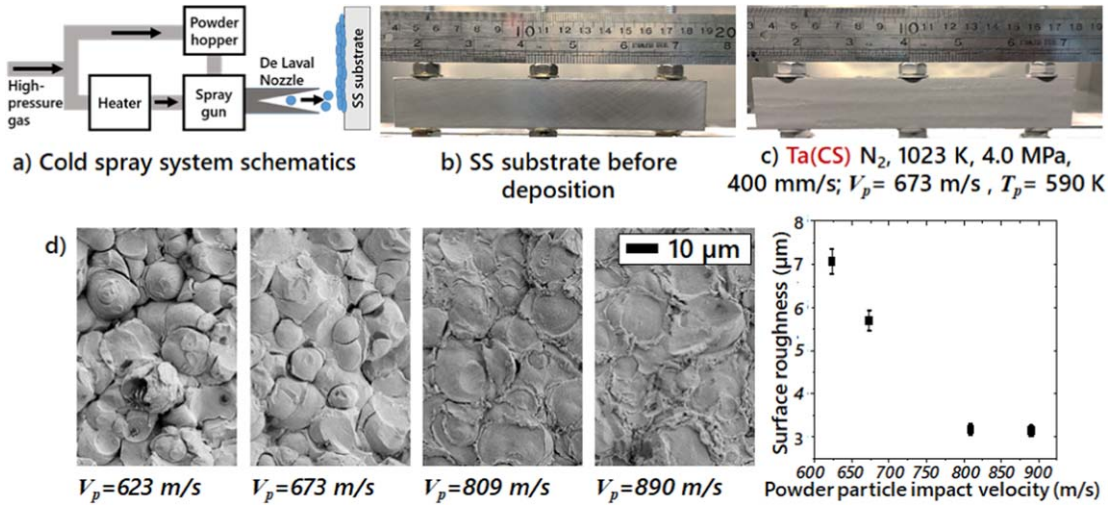

Figure 3. (a) Schematic illustration of the cold spray system, photograph of 316L stainless-steel substrate plate (b) before and (c) after deposition of tantalum. (d) SEM images and roughness of the surface of as-sprayed Ta coatings for different particle impact velocities V_p.

2.2. Plasma irradiation experiments and annealing tests

After deposition, a sample with a square shape of 10×10 mm^2 was sectioned from the Ta-coated SS 316L plate using the wire EDM method. This sample is henceforth referred to as Ta(CS). The sample was mechanically polished to mirror-like surface finish (roughness <0.5 μm) to remove roughness effects inherent to the cold spray process and obtain the uniform surface condition across the sample in order to reduce uncertainties related to roughness effects. A bulk vacuum-arc cast (not cold sprayed) Ta sample (Eagle Alloys Corp., 99.96% purity, annealed at 1370 K) identified as Ta(B) and a bulk polycrystalline tungsten sample (ALMT corp., 99.95% purity, annealed at 2073 K) identified as W(B) were also prepared in the same manner and served as base-line reference. The three samples were simultaneously irradiated in a deuterium plasma in the linear plasma device PSI–2 (Jülich, Germany) [28]. The typical incident D kinetic energy was 95eV, which is, below the threshold energy for sputtering of Ta by D (see figure 1 and [29]). Prior to D irradiation, the samples were outgassed at 800K for 10 minutes by a resistive heater installed on the sample stage under the samples and then cooled down to 530 K by a combination of heater control and water cooling capabilities of the sample stage. During the ~143 minutes plasma exposure in the PSI-2, the heater was turned off as the samples were heated by the plasma itself. A thermographic measurement system in PSI–2 showed nearly constant temperature of ~530 K of the samples during the exposure. The incident D flux measured by the reciprocating Langmuir double probe was 3.5×10^{21} D m^{-2} s^{-1} and the total incident fluence was 3×10^{25} D m^{-2}. Just after irradiation, the samples were cooled down to room temperature (RT) within a few minutes. Oxygen is the main impurity in PSI–2 plasma and is on the order of 0.1% [30] leading to a negligible sputtering contribution from the plasma background. Detailed information about the layout of the PSI–2 device, its parameters and operational conditions can be found in [28].

After the D plasma irradiation, the W(B), Ta(B) and Ta(CS) samples were introduced into the ultra-high vacuum CAMITER system (base pressure $<2.3 \times 10^{-7}$ Pa) capable of performing high-sensitivity thermal desorption spectrometry (TDS) measurements at the PIIM laboratory of Aix-Marseille University (Marseille, France). In this experiment, the samples were heated at a rate of 0.5 K s^{-1} up to 1100 K, held for 15 minutes at this temperature and then allowed to cool down to room temperature. During this annealing, a multiplexed Quadrupole Mass Spectrometer (QMS) was used to record simultaneously the outgassing of HIs molecules, i.e. of HD and D_2. Time integration of the recorded QMS spectra allowed to evaluate the deuterium desorption from the three samples.

2.3. Characterization of samples

Surface roughness evaluation was performed on the three samples using a S neox laser confocal microscope from SENSOFAR located at the PIIM laboratory.

Further characterization of the Ta coating and Ta bulk samples was performed at the Wisconsin Centers for Nanoscale Technology. Surface and cross-sectional scanning electron microscopy (SEM) analysis was performed on Ta(CS) after each of the following steps: (i) Ta cold spray deposition and mechanical polishing, (ii) D irradiation, and (iii) after annealing. This approach allowed to evaluate the morphological changes in the cold

spray coating related to the effects of D irradiation and thermal treatment at the elevated temperature. SEM was performed in a Zeiss/Gemini 450 microscope coupled with a Thermo Noran x-ray electron dispersive spectroscopy (EDS) for elemental identification.

High-resolution compositional analysis of the surface and subsurface regions was conducted on the samples after each experimental step using Thermo K alpha x-ray photoelectron spectrometer (XPS). The XPS system is equipped with monochromatic Al k-alpha x-ray source for high resolution XPS analysis on a spot size of 400 μm. The base pressure during XPS analysis was $\sim 3 \times 10^{-5}$ Pa. Additionally, depth profiling study was performed on the D-irradiated samples utilizing 2 keV argon (Ar) ion beam sputtering system of the XPS apparatus. The x-ray source was operated at 12 kV and 3.25 mA. The spectra were collected with an analyzer pass energy of 50 eV and step size of 0.025 eV. Shirley background subtraction and peak fitting with Gaussian-Lorentzian-shaped profiles was performed using Thermo Scientific^{TM} Avantage software. O1s and C1s peaks signals were also collected and used as the reference binding energies.

The phases in the samples were verified with x-ray diffraction (XRD) using a Bruker D8 Discovery x-ray diffractometer equipped with Cu-Kα micro x-ray source ($\lambda = 0.1542$ nm).

3. Results and discussion

3.1. Powder particle impact in the cold spray

In cold spray process, the velocity of the impacting powder particles has the most dominant effect of the coating structure and properties [31]. The particle velocity in turn depends on factors such as propellent gas mixture composition, gas preheat temperature, and particle size and density. In our study, ANSYS Fluent software was used to simulate supersonic gas flow through the converging-diverging nozzle. The flow of the carrier gas through the nozzle was modeled as a 2D, isentropic, single-phase flow. A species transport model with volumetric reaction and eddy dissipation was applied for the gas mixtures used in this study. A single tantalum particle was introduced into the gas stream to predict its velocity V_p and temperature T_p as it flows through the nozzle. Computational fluid dynamics was used to simulate the flow behavior of the gas mixture and particle through the nozzle by considering parameters such as the mass, density, and cross-sectional area of the particle and the drag coefficient for a sphere. The convective heat transfer between the carrier gas and the particle was also considered [32]. The parameters used for cold spraying the sample for this study and the resulting values of the velocity V_p and temperature T_p of the tantalum particles at the outlet of the nozzle are reported in figure 3 (c). Figure 3 (d) shows that the surface morphology of coatings is strongly dependent on the powder particle velocity: Ta particles experience more plastic deformation with an increase in V_p which results in a denser deposition and reduced surface roughness. Since the maximum temperature of the particles at the nozzle outlet is about 590 K, no significant change in mechanical properties of powder particles is expected [33].

Figure 4(a) shows a typical cross-sectional SEM image of the Ta(CS) sample after deposition. The deposited coating appears uniformly dense and free of any micro-scale pores through the entire thickness of 302 ± 41 μm. The interface between the coating and the substrate does not exhibit any effects of delamination. Figure 5(a) shows the surface of Ta(CS) sample after mechanical polishing prior to D irradiation.

3.2. Effects of D irradiation and annealing tests

3.2.1. Microstructure of the coatings

Figure 4(b) shows that exposure to the high fluence of D and subsequent thermal annealing at 1100 K for 15 minutes did not induce any microstructural changes in the bulk and subsurface regions of the coating. A high magnification SEM image of the interface between the coating and the substrate presented in figure 4(c) qualitatively indicates the integrity of the bonding between the tantalum coating and the SS 316L substrate. SEM observation also reveals the presence of inter-particle boundaries which suggests that porosity may be present in the coating at smaller (nanometer) length scales. Post-annealing examination suggests that the cold spray Ta coating produced using the particle velocity of $V_p = 673$ m/s has a potential to withstand high temperature cycling.

To evaluate the effects of high-fluence D irradiation and thermal annealing on the Ta(CS) coating surface, we took advantage of a single stainless steel impurity particle with the size of ~ 1500 μm^2. This particle was likely introduced as an artifact of sample preparation since only a very few of these particles were observed on the entire surface area of the sample. This artifact stainless steel particle reference area was investigated with SEM at each step of the experiment. Figure 5 (c) shows a SEM image of the surface of the Ta(CS) sample after mechanical polishing to the mirror-like surface finish (roughness <0.5 μm) featuring the Ta surface (bright contrast) and a stainless steel particle surface (dark contrast) embedded in the coating. The small black dots and striations on the Ta regions highlighted with the blue line are likely micropores in the Ta coating and the region encircled in red

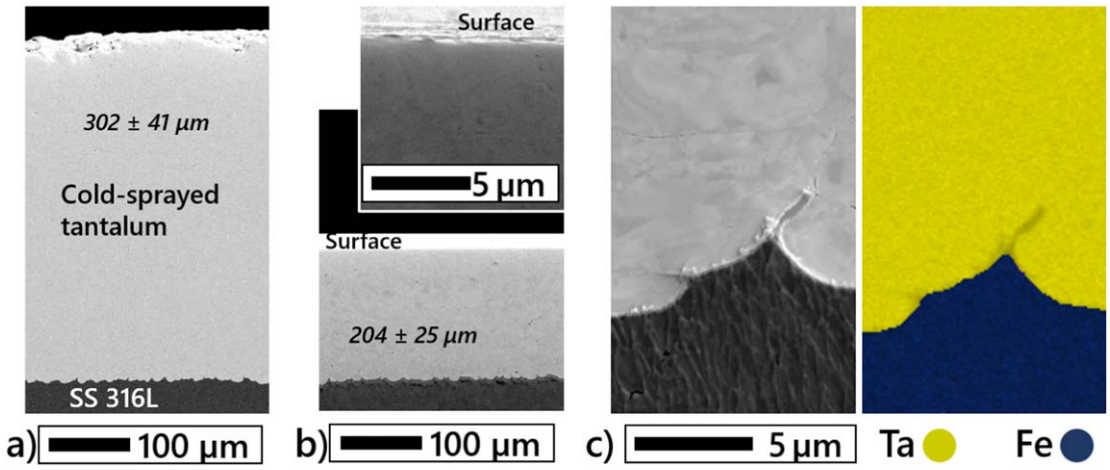

Figure 4. Cross-sectional SEM images of the cold sprayed sample (a) after deposition and (b) after the sample was mechanically polished, irradiated with 95 eV deuterium ions and annealed at 1100 K for 15 minutes (the inset shows the area close to the surface). Thicknesses of coating for the two cases is also indicated. (c) A close-up view of the interface between tantalum cold spray and SS 316L substrate and the EDS map of the same area after the annealing experiment.

highlights the slightly separated particle-to-particle interface [10]. These defects could have originated in the coating surface produced during the sample preparation procedures.

Figure 5(d) shows the same area on the Ta(CS) sample surface after irradiation with 95 eVD ions at a fluence of 3×10^{25} D m^{-2} at 535 K. D irradiation did not induce any noticeable changes on the surface of Ta which is in agreement with results reported in literature [14]. Surface and cross-sectional analysis on the coating confirmed absence of surface blisters (see also the SEM observations of the large surface areas before and after D irradiation in figures 5(a) and (b)) which is in contrast to the high-dosage irradiation in W where the surface temperature is below the desorption temperature of D (~500 K) and severe damage effects were observed [34]. Our experiments highlight the excellent resistance of the cold sprayed Ta to the high-fluence low-energy D irradiation similar to the bulk Ta material [14].

However, as expected, 95 eV D ion bombardment at 535 K caused significant surface damage to stainless steel, the main compositional element of which is iron (Fe). Differential sputtering of Fe by the incident D ions appears to be the cause of the observed morphological changes in the stainless steel region since the sputtering yield for Fe at this energy is 0.0033% [29]. Subsequent annealing of the Ta(CS) sample at 1100 K for 15 minutes did not change the surface morphology of the cold sprayed Ta, but some smoothing of the damaged stainless-steel surface was observed as shown in figures 5(e) and (f).

3.2.2. Effects of D implantation and annealing on compositional and structural changes in cold sprayed tantalum

Figure 6(a) shows the total amounts of outgassed deuterium (as a measure of deuterium retention), for the bulk W, bulk Ta and cold spray Ta samples during the annealing experiment up to 1100 K: $(7.5 \pm 0.1) \times 10^{21}$ D/m^{-2} from W(B) sample, $(1.0 \pm 0.1) \times 10^{24}$ D/m^{-2} from Ta(B) sample, $(3.1 \pm 0.2) \times 10^{24}$ D/m^{-2} from Ta(CS) sample. This corresponds to outgassing of 0.03% (W(B)), 3.4% (Ta(B)) and 10.3% (Ta(CS)) respectively of the initial deuterium irradiation fluence. The quantity released from W(B) correlates with the expected deuterium retention in non-damaged polycrystalline tungsten [35, 36]. The quantity released from Ta(B) is almost 2 orders of magnitude higher than from W(B) which confirms the expected high D trapping capability of tantalum. Moreover, the desorption results for the cold spray Ta reveal the enhanced D release from the coating which constitutes 30% of the SRIM predicted implantation probability for D in Ta under our irradiation conditions (the dashed line in figure 6(a)). High retention in tantalum cold spray coating is likely related to the surface and bulk microstructure of Ta(CS) material.

XRD structural analysis performed on the tantalum samples before plasma exposure experiment revealed the characteristic scattering peaks of the α-phase of Ta with the lattice parameter of 3.3068 Å (see figure 6(b)). The differences in the relative peak intensities of the pristine Ta(CS) and Ta(B) samples originate from the differences in the manufacturing route used for the preparation of these samples [37]. D irradiation of the cold sprayed tantalum induced a slight increase in the lattice parameter to 3.3185 Å, which is within the uncertainty of the measurement, but it could also be indicative of D embedding in the tantalum lattice. However, we note on the absence of additional peaks corresponding to the formation of a tantalum hydride phase [20] which is likely due to their concentration limits being below the detection limits of XRD. Finally, annealing of the sample at

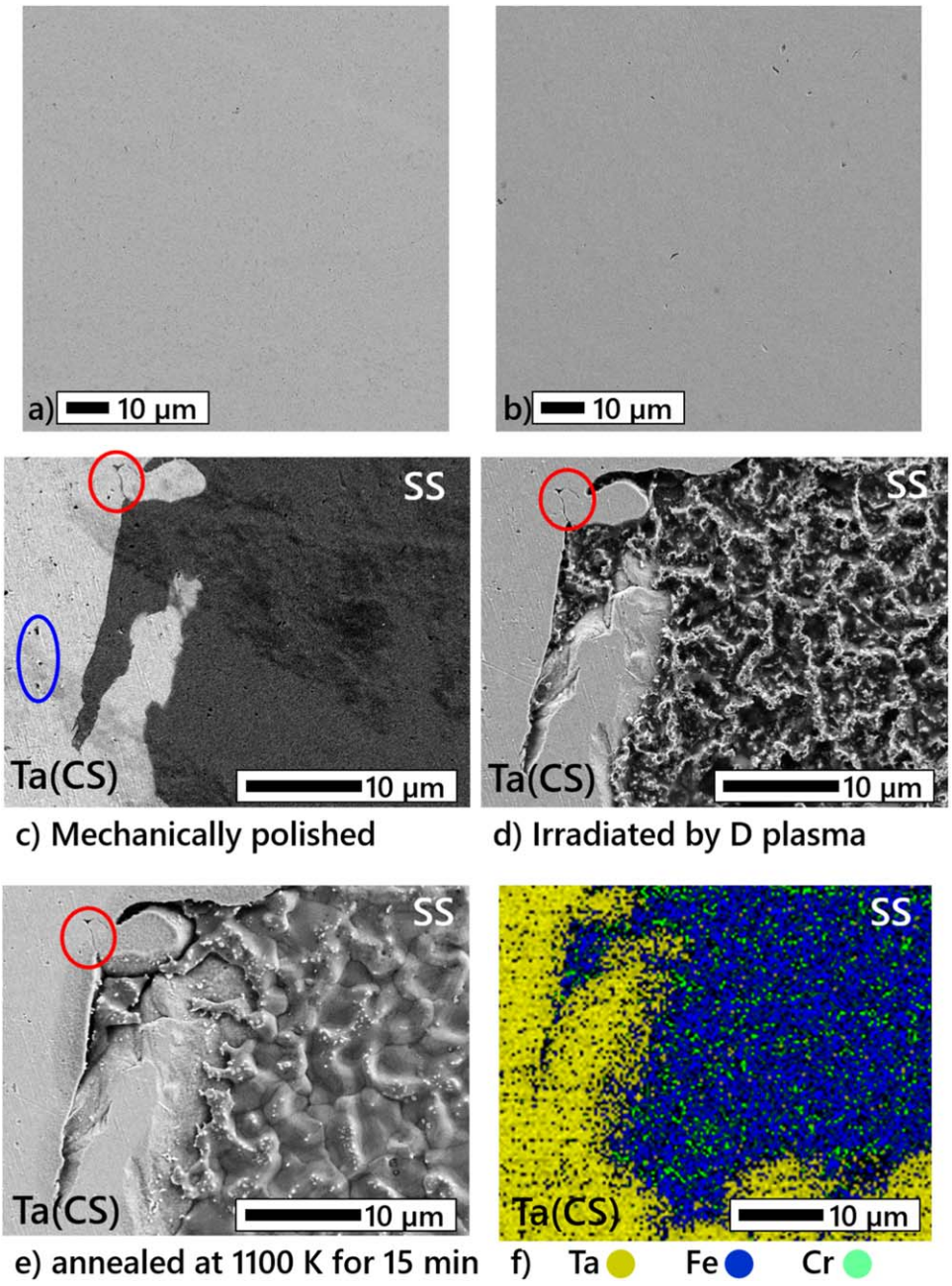

Figure 5. SEM images of the surface of the cold sprayed tantalum Ta(CS) sample with a stainless-steel impurity particle (a) and (b) before irradiation, (c) and (d) after irradiation with 95 eV deuterium ions at 535 K. (e) SEM image and (f) EDS map of the same area after annealing at 1100 K for 15 minutes.

1100 K led to the recovery (shrinkage) of lattice parameter to the original value after D outgassing confirming the structural stability of the coating which is not affected by the high temperature exposure.

The black curve in figure 6(c) shows the XPS 4f domain spectrum of the mechanically polished Ta(CS) and Ta(B) samples (thick and thin black curves respectively) prior to D plasma irradiation. The spectra of these pristine samples feature two pairs (doublets) of peaks: the metallic doublet Ta $^{0}_{(7/2)}$ at 21.60 eV and Ta $^{0}_{(5/2)}$ at 23.50 eV, and the tantalum pentoxide Ta_2O_5 doublet Ta $^{5+}_{(7/2)}$ at 26.79 eV and Ta $^{5+}_{(5/2)}$ at 28.70 eV. Ta_2O_5 is the most stable Ta-oxide state [27].

Irradiation with 95 eV D ions at 535 K resulted in significant evolution in the XPS spectrum highlighting a change of the near-surface composition (red curves in figure 6 c)). Firstly, the metallic signature of Ta is suppressed by the presence of low oxidation states Ta^{1+}, Ta^{2+}, Ta^{3+}, Ta^{4+}. Ta^{5+} doublet appears slightly red-shifted by 0.3 eV in both samples. It is important to note that no oxide growth was observed with SEM on the surface and cross-section of our samples, and additionally, oxidation has not been previously reported after D plasma irradiation experiments in the PSI-2 device.

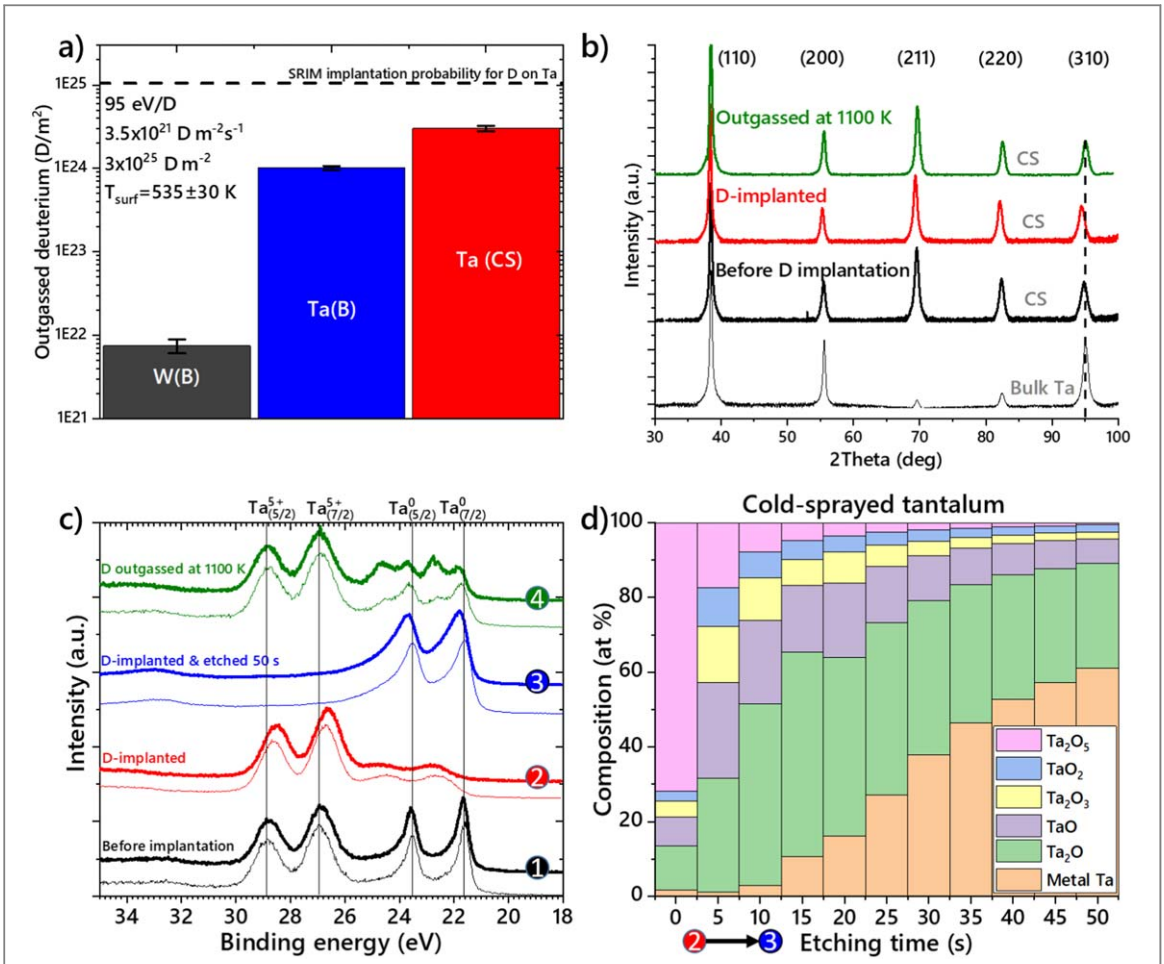

Figure 6. (a) Thermo-Desorption Spectrometry results for the bulk tungsten W(B), the bulk tantalum Ta(B) and cold sprayed tantalum Ta(CS) samples. (b) x-ray diffraction (XRD) patterns of the Ta(CS) sample at each stage of the experiments. Thin curve shows the XRD spectrum of the Ta(B) prior to D implantation. (c) XPS spectra of the Ta(B) (thin curves) and Ta(CS) (thick curves) samples and (d) results of depth profiling study using 2 keV argon ions on Ta(CS) implanted with deuterium.

In order to investigate the chemical states of D-implanted tantalum, Ta(CS) and Ta(B) samples were sputter cleaned (etched) using 2 keV Ar ions and 11 spectra were recorded over 50 seconds of the total etching time until the collected XPS spectra did not show any further evolution. Each individual spectrum was fitted considering metallic and all oxide contributions following the procedure described by Simpson *et al* [38]. The FWHM of the peaks fitted to the spectra after sputter cleaning were allowed to increase to accommodate ion beam induced broadening.

Figure 6(d) presents the results of the depth profiling spectra deconvolution for the Ta(CS) sample featuring a gradual increase of metallic Ta contribution and a decrease of the oxide state contributions with the 50seconds of sputtering time. Etching for longer times did not completely remove the oxide layer from the surface owing to the lesser passivation characteristics of Ta. Interestingly, Ta^0 doublet of the coating appears blue-shifted by 0.5 eV while the metallic doublet of the bulk sample is restored to its reference position at 21.60 eV and 23.50 eV after sputter cleaning. While the observed broadening of the spectrum can be attributed to the ion beam induced change in surface roughness and defect creation [38], the reasons for the shift of the electron binding energy of the metal doublet of the coating can not be fully interpreted in the present study. We speculate that this observation may be associated with the presence of deuterium in Ta and is indicative of the formation of Ta-D bonds (tantalum deuteride), similar to the phenomena observed in titanium hydrides [39]. This hypothesis also explains the observed shift of the Ta^{5+} doublet after plasma irradiation since saturation of the surface oxide with D should reveal a chemical shift in the XPS spectrum. Saturation of the tantalum samples with D to a high atomic ratio may help to validate this hypothesis.

XPS analysis of the surface of the samples after annealing at 1100 K for 15 minutes (green curves in figure 6 (d)) revealed a recovery of the metallic Ta and Ta_2O_5 peaks and an appearance of the additional doublet at 22.76 eV and 24.67 eV. The new doublet is stable after air exposure and an additional annealing cycle up to 1100 K and is attributed to either a lower oxidation state or due to deuteride presence in Ta.

It is worth noting that although the Ta powder particles feature some surface oxidation (see figure 2), our XPS study revealed a very similar composition and its evolution after each experimental step between the cold sprayed and bulk Ta samples. This suggests that the native oxide layer on the particles' surfaces was jetted out by the high energy impact during the cold spray deposition which minimizes oxide presence on the surface and in the inter-particle boundaries of the coating.

4. Conclusions and outlook

This work reports the results of an initial study on development of cold spray coated tantalum first-wall interface for fusion applications for trapping hydrogen isotopes and with capabilities of withstanding low-energy high-fluence deuterium irradiation and temperatures up to 1100 K.

Cold spray deposition technology was used to deposit thick tantalum coating on 316L stainless-steel substrate. Based on modeling for the set of cold spray parameters used in this study, the velocity of the impacting powder particles was determined to be about 673 m/s. Scanning electron microscopy cross-sectional examination revealed the coating to be dense but with a fine-scale porosity, and a good adhesion to the substrate.

Irradiation of the coatings with 95 eV deuterium ions at 535 K at the dose of 3×10^{25} D m^{-2} did not affect the surface or bulk microstructure of the coating at the microscale. Thermal desorption analysis revealed a 3 times higher deuterium release from the cold sprayed Ta coatings compared to the bulk tantalum, and 2 orders of magnitude higher deuterium retention compared to the polycrystalline tungsten.

Compositional and structural analysis linked with deuterium retention analysis performed after plasma irradiation and subsequent annealing at 1100 K for 15 min indicated embedding of deuterium in the tantalum lattice and subsequent release of deuterium after annealing. In general, the behavior of cold sprayed tantalum is similar to bulk Ta in regards to structural and compositional evolution upon D irradiation and exposures up to 1100 K. These characteristics demonstrate the suitability of the cold spray tantalum coatings for deuterium trapping and regeneration for the applications in small-scale fusion devices. It is expected that the nanoscale porosity in the cold spray coating provides an additional mechanism for enhanced trapping of deuterium. The porosity level in tantalum coatings can be controlled quite readily by changing the cold spray parameters. The effect of the microstructure and the role of fine-scale defects on deuterium retention in the cold spray is the subject of the next phase of our study.

Acknowledgments

The information, data, or work presented herein was funded in part by the Advanced Research Projects Agency-Energy (ARPA-E), U S Department of Energy, under Award Number DE-AR0001258; in part by the U S Department of Energy under grant DE-SC0020284 and by directfundsof the College of Engineering and the Department of Nuclear Engineering and Engineering Physics at the University of Wisconsin—Madison. The views and opinions of authors expressed herein do not necessarily state or reflect those of the United States Government or any agency thereof.

The authors gratefully acknowledge use of facilities and instrumentation at the UW-Madison Wisconsin Centers for Nanoscale Technology (wcnt.wisc.edu) partially supported by the NSF through the University of Wisconsin Materials Research Science and Engineering Center (DMR-1720415).

A part of this work has been carried out within the framework of the French Federation for Magnetic Fusion Studies (FR-FCM). The authors are thankful to Dr. Celine Martin for providing access to the Confocal microscope at the PIIM laboratory of the Aix-Marseille University and for valuable discussions and suggestions on the research presented in this paper.

Data availability statement

All data that support the findings of this study are included within the article (and any supplementary files).

ORCID iDs

Mykola Ialovega https://orcid.org/0000-0003-0041-8039
Tyler Dabney https://orcid.org/0000-0002-8058-8996
Régis Bisson https://orcid.org/0000-0002-8819-1563
Arkadi Kreter https://orcid.org/0000-0003-3886-1415
Oliver Schmitz https://orcid.org/0000-0002-9580-9149

References

[1] Redhead P A 1999 Extreme high vacuum *CAS—CERN Accelerator School: Vacuum Technology* vol 05 (CERN)
[2] Redhead P A 2003 *AIP Conf. Proc.* **671** 243–54
[3] Egedal J, Endrizzi D, Forest C and Fowler T 2022 *Nucl. Fusion* **62** 126053
[4] Anderson D T *et al* 2006 *Fusion Sci. Technol.* **50** 171–6
[5] Kumar S, Vidyasagar V, Jyothirmayi A and Joshi S V 2016 *J. Therm. Spray Technol.* **25** 745–56
[6] Grujicic M 2007 9 - Particle/substrate interaction in the cold-spray bonding process *The Cold Spray Materials Deposition Process Fundamentals and Applications* ed V K Champagne (Woodhead Publishing) pp 148–77
[7] Richou M, Chu I, Darut G, Maestracci R, Ramaniraka M and Meillot E 2022 *Journal of Nuclear Engineering* **3** 453–60
[8] Neu R, Maier H, Böswirth B, Elgeti S, Greuner H, Hunger K, Kondas J and von Müller A 2023 *Nuclear Materials and Energy* **34** 101343
[9] Cardonne S, Kumar P, Michaluk C and Schwartz H 1995 *Int. J. Refract. Met. Hard Mater* **13** 187–94
[10] Jafarlou D M, Sousa B C, Gleason M A, Ferguson G, Nardi A T, Cote D L and Grosse I R 2021 *Additive Manufacturing* **47** 102243
[11] Koivuluoto H, Näkki J and Vuoristo P 2009 *J. Therm. Spray Technol.* **18** 75–82
[12] Takagi I, Nagaoka S, Shirai K, Moritani K and Moriyama H 2003 *Phys. Scr.* **2003** 121
[13] Asakawa T, Nagano D, Miyazawa H and Clark I 2020 *Journal of Vacuum Science & Technology* B **38** 034008
[14] Novakowski T, Sundaram A, Tripathi J, Gonderman S and Hassanein A 2018 *J. Nucl. Mater.* **504** 1–7
[15] Luo J, Tuo F and Kong X 2009 *Phys. Rev.* C **79** 057603
[16] Szabo P, Weichselbaum D, Biber H, Cupak C, Mutzke A, Wilhelm R and Aumayr F 2022 *Nucl. Instrum. Methods Phys. Res., Sect. B* **522** 47–53
[17] Koivuluoto H, Honkanen M and Vuoristo P 2010 *Surf. Coat. Technol.* **204** 2353–61
[18] Delloro F, Jeandin M, Jeulin D, Proudhon H, Faessel M, Bianchi L, Meillot E and Helfen L 2017 *J. Therm. Spray Technol.* **26** 1838–50
[19] 2012 Residual stress measurements of cold sprayed tantalum coatings
[20] Iturbe-Garcia J and Lopez-Munoz B 2014 *Advances in Nanoparticles* **3** 159–66
[21] Kuzovnikov M A, Tkacz M, Meng H, Kapustin D I and Kulakov V I 2017 *Phys. Rev.* B **96** 134120
[22] Simonovic B R, Mentus V S and Dimitrijevic R Z 2003 *J. Serb. Chem. Soc.* **68** 657–63
[23] Wampler W R 1991 *Journal of Vacuum Science & Technology* A **9** 1334–9
[24] Yoshida N and Hirooka Y 1998 *J. Nucl. Mater.* **258-263** 173–82
[25] Setyowati V A, Suheni, Widodo E W R and Hermanto S A 2019 *IOP Conference Series: Materials Science and Engineering* **462** 012012
[26] Pitts R *et al* 2013 Proceedings of the xx international conference on plasma-surface interactions in controlled fusion devices *J. Nucl. Mater.* **438** S48–56
[27] Novakowski T J, Tripathi J K and Hassanein A 2016 *Sci. Rep.* **6** 39746
[28] Kreter A, Brandt C, Huber A, Kraus S, Möller S, Reinhart M, Schweer B, Sergienko G and Unterberg B 2015 *Fusion Sci. Technol.* **68** 8–14
[29] Eckstein W, Garciá-Rosales C, Roth J and László J 1993 *Nucl. Instrum. Methods Phys. Res., Sect. B* **83** 95–109
[30] Schmitz J *et al* 2018 *Nuclear Materials and Energy* **15** 220–5
[31] Dykhuizen R C and Smith M F 1998 *J. Therm. Spray Technol.* **7** 205–12
[32] 2012 On simulation of multi-particle impact interactions in the cold spray process (International Joint Tribology Conference vol ASME/STLE 2012 International Joint Tribology Conference)
[33] Škoro G, Bennett J, Edgecock T, Gray S, McFarland A, Booth C, Rodgers K and Back J 2011 *J. Nucl. Mater.* **409** 40–6
[34] Wang W, Roth J, Lindig S and Wu C 2001 *J. Nucl. Mater.* **299** 124–31
[35] Roszell J, Davis J and Haasz A 2012 *J. Nucl. Mater.* **429** 48–54
[36] Bisson R, Markelj S, Mourey O, Ghiorghiu F, Achkasov K, Layet J M, Roubin P, Cartry G, Grisolia C and Angot T 2015 *J. Nucl. Mater.* **467** 432–8
[37] Jakubowicz J, Adamek G and Sopata M 2017 *IOP Conference Series: Materials Science and Engineering* **216** 012006
[38] Simpson R, White R G, Watts J F and Baker M A 2017 *Appl. Surf. Sci.* **405** 79–87
[39] Tsuchiya B, Oku M, Sahara R, Nagata S, Shikama T and Kawazoe Y 2008 *Journal of Surface Analysis* **14** 424–7